EVALUATION OF URBAN SCALE CONTAMINANT TRANSPORT AND DISPERSION MODELING USING LOOSELY COUPLED CFD AND MESOSCALE MODELS

William J. Coirier [*], Sura Kim
CFD Research Corporation, Alabama
Fei Chen, Mukul Tewari
National Center for Atmospheric Research, Colorado

1. INTRODUCTION

As noted in [OFCM, 2004], there exists a scale gap between the micro (urban) and meso scales, and in [Marshall, 2004] the close coupling between mesoscale model uncertainty and urban scale transport and dispersion modelling accuracy is brought forth. This paper assesses one option that may be taken to close this gap and address this uncertainty; one-way coupling between a microscale Computational Fluid Dynamics (CFD) model and a mesoscale Numerical Weather Prediction (NWP) model. There are many advantages of a loose, quasi-static coupling as opposed to a tighter, temporal-based coupling, which are noted in subsequent sections. In this paper we assess these couplings and the effect of the downscale data transfer (from meso to urban scale) upon the microscale area transport and dispersion modeling accuracy.

Both modeling scales lack information that the other needs. Urban scale motions are influenced in part by the larger and slower atmospheric forcings, but computations in the urban scale rarely use this information. Urban scale calculations often apply simplistic boundary conditions, and rarely, if ever, apply body force terms related to a mesoscale forcing. At the urban scale the use of measured data from soundings and meteorological stations is quite often incomplete and inconsistent and is usually available at limited locations, and are quite often not even near the area of interest. This lack of information is becoming more of a problem recently, since the computational power available on the desktop level is rapidly increasing, allowing much larger urban scale domains to be effectively simulated. Applying boundary conditions that do not vary laterally across the domain becomes more unrealistic as the urban scale domain sizes increase into the many kilometers of range.

The influence of the urban scale upon the mesoscale is also very important, including such coupled behavior as an increased drag force caused by the buildings, which in turn causes a larger Ekman turning. This can cause the flow direction above the city to be significantly different than the lower level winds, which has a direct impact upon contaminant transport and dispersion in the city. Many important processes at the urban scale can impact the mesoscale, including: urban-scale surface inhomogeneities causing heat islands, thermally driven mesoscale scale circulations, and enhanced convergence zones. Differential heating and trapping of heat can also affect the atmospheric structures and larger scale flows. Modeling of these small scale features economically and accurately is difficult, and is the subject of much research.

In this paper, we will demonstrate the down-scale transfer of data from a mesoscale NWP model to an urban scale model, and quantifiably assess the impact of this down-scale transfer upon the urban scale transport and dispersion modeling accuracy. Two different modes of transferring this data from the mesoscale model to the urban scale model have been addressed; an unsteady and a quasi-steady mode. The two approaches are assessed by computing statistical measures representing the accuracy of the transport and dispersion of a tracer gas, SF_6, corresponding to an Intensive Operating Period (IOP) of the Urban 2000 Field Test in Salt Lake City [Allwine 2002]. In the following, we briefly describe each model, the coupling strategies, the experiment and the results of the assessment. A recommendation is then made as to how best to couple these two types of models, where an operational, loosely coupled scheme is outlined that is based upon the quasi-steady model.

---

corresponding author address:
CFD Research Corporation,
215 Wynn Dr., 5th Floor, Huntsville, AL 35805
e-mail: wjc@cfdrc.com.

2. MICROSCALE MODEL: CFD-Urban

CFD-Urban is a suite of Computational Fluid Dynamics modeling software that is being used to simulate the wind, turbulence and dispersion fields in urban areas [Coirier et al., 2003.a, 2005.b]. CFD-Urban has been developed under a program sponsored by the Defense Threat Reduction Agency [Coirier et al., 2003.b, 2005.a], and has been built using parts of a commercially available software suite, CFD-ACE+ [ACE+ 2003]. It solves the Reynolds-Averaged Navier-Stokes equations using a collocated, Finite-Volume method implemented upon structured, unstructured and adaptively-refined grids using a pressure-based approach based upon the SIMPLE algorithm [Jiang, 1994, Jiang, 1999]. Turbulence closure is found by solving a variant of the standard k-ε model [Launder, 1974]. Buildings are modeled either explicitly, by resolving the buildings themselves, and/or implicitly, by modeling the effects of the buildings upon the flow by the introduction of source terms in the momentum and turbulence model equations [Coirier 2003.b]. CFD-Urban solves the steady-state and unsteady Reynolds Averaged Navier-Stokes (RANS) equations, as well as by using a Large Eddy Simulation (LES) approach. Since CFD-Urban solves the governing mass and momentum conservation laws at scales smaller than the buildings themselves, important urban aerodynamic features are naturally accounted for, including effects such as channeling, enhanced vertical mixing, downwash and street level flow energization.

3. MESOSCALE MODEL: WEATHER RESEARCH AND FORECASTING MODEL (WRF)

The Weather Research and Forecast (WRF) modeling system was applied to the complex urban environment over the Salt Lake City (SLC) region to provide initial and lateral boundary conditions for CFD-urban. WRF is a joint development effort between NCAR, government agencies including the DOD and the university research community. The WRF model provides a common framework for both research and operational numerical weather prediction. WRF is a completely redesigned code, has superior numerics, targeted for the 1-10 km grid-scale and intended for operational weather forecasting, regional climate prediction, air-quality simulation, and idealized dynamical studies. In this project, we used the research-quality version of the WRF model with nesting capability (WRF V2.0) released in May 2004. The particular models used for this study are described fully in subsequent sections.

4. MODEL ASSESSMENT: URBAN 2000, IOP 10

We have used the URBAN 2000 Field Test data from Intensive Operating Period (IOP) 10 [urban.llnl.gov] to quantifiably measure the accuracy of the transport and dispersion modeling using different coupling strategies of ingesting the downscale data from WRF. IOP10 was performed on October 25 to October 26, 2000. Meteorological and gas sampler data is available that nominally covers the period 1200 MST October 25, 2000 (DOY 299) through 1200 MST October 26, 2000 (DOY 300). SF_6 was released three times over the entire IOP, with the release "on" for 1 hour, and then "off" for one hour, for a total period of 6 hours. The calculations we have performed here use this same release schedule and source strength, covering the entire IOP 10.

4.1 WRF Model Systems Configuration

The WRF modeling systems that were used for this study had the following configuration: Non-hydrostatic dynamics, two-way interactive nesting procedure, radiative upper-boundary condition, time-dependent lateral-boundary conditions, relaxed toward large-scale model forecasts, new Kain-Fritsch [Kain and Fritsch 1993] cumulus parameterization on 10 km grid-increment, or larger, grids, [Liu et al., 1996] mixed-phase ice scheme, Mellor-Yamada-Janjic TKE level 2.5 [Janjic, 2002] planetary boundary-layer parameterization, cloud-radiation scheme of Dudhia [1989]] for shortwave and the Rapid Radiative Transfer Model [Mlawer et al. 1997] for longwave, Noah land-surface model (a modified Oregon State University land-surface model, [Chen and Dudhia 2000]),

Two types of urban parameterization schemes were used in the WRF/Noah coupled system. : 1) a simple urban treatment in the Noah LSM [Liu et al., 2005], and 2) a coupled Noah / urban canopy model (UCM), which is currently in development and based on the single-layer UCM of Kusaka et al. (2001). These integrated WRF/Noah/UCM and WRF/Noah models were configured with five two-way interactive nested grids having grid spacing of 40.5,13.5,4.5,1.5, and 0.5 Km. They employed 31 vertical levels with 16 levels within the lowest 2 km. The WRF model was initialized at 00 UTC 26 October 2000 (IOP-10 period) and applied to

perform a 24-h simulation. The initial and lateral boundary conditions for WRF was supplied by analyses and forecast from the NCEP Eta data assimilation system (EDAS).

4.2 Dispersion Modeling Accuracy

The transport and dispersion modelling accuracy assessment is made using standard statistical measures, as proposed by [Weil et al., 1992], and used previously by many transport and dispersion model validation and verification studies [Coirier et al., 2004].

$$FB = \frac{\left(\overline{C_o} - \overline{C_P}\right)}{\left(\overline{C_o} + \overline{C_P}\right)/2} \tag{1}$$

$$MG = \exp(\overline{\ln C_o} - \overline{\ln C_P}) \tag{2}$$

$$NMSE = \frac{\overline{(C_o - C_P)^2}}{\overline{C_o}\,\overline{C_P}} \tag{3}$$

FAC2=fraction of $\dfrac{1}{2} \le \dfrac{C_P}{C_O} \le 2$ (4)

Where C_P, C_O are the predicted and observed concentrations, respectively. In the equations above, the averaging operator is taken over samplers located in four groupings (arcs), as shown in Figure 1: Near source, R2, R3 and R4, corresponding to the CBD, 2km, 4km and 6km arcs in the field test.
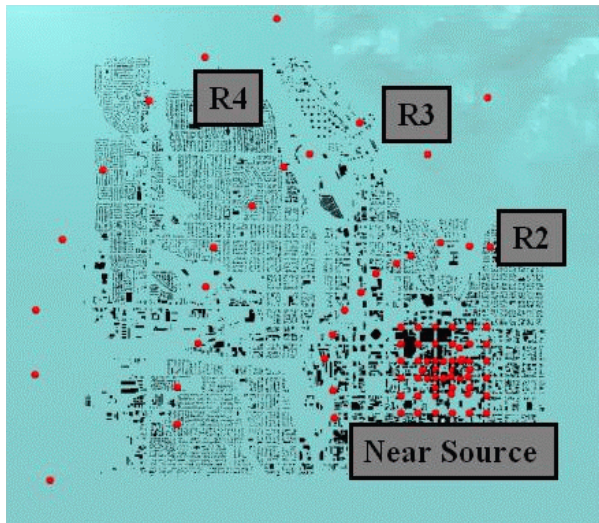
Figure 1: Sensor Arcs used in statistical measures.

4.3 Coupling Strategies

As noted above, WRF data is made available via NetCDF files at 15 minute intervals, spanning the IOP10. Two different strategies of coupling the CFD and mesocale models have been addressed: An unsteady approach and a "quasi-steady" approach. Both of these spatially interpolate data from the WRF data files using the following procedures.

Spatial Interpolation of WRF Data

The WRF data files, in NetCDF format [NetCDF], are processed to produce files in the Data Transfer Facility (DTF) format [Coirier, W.J., 1998]. WRF uses a staggered grid approach (Arakawa C-staggering), where thermodynamic data are stored at the cell-centers of the mesh, and the velocity field is stored at the face-centers of the mesh. In order to simplify the interpolation procedures, we average the velocity components to the cell centers. Furthermore, we store the mesh dual (cell-centers) as nodes in the DTF file representation, which simplifies both visualization and processing of the data, since all data stored at the same location. The field data is spatially interpolated from the hexahedral WRF cells to the individual face centroids in the CFD mesh using a continuous, linear interpolant. The particular data read in from WRF includes the velocity components, pressure base state and perturbation potential, temperature, turbulence kinetic energy from the Mellor-Yamada-Janjic [Mellor, et al., 1974] model and the momentum diffusion coefficient. The turbulence kinetic energy dissipation rate for the k-ε model is found from the definition of the diffusion coefficient:

$$\varepsilon = \rho C_\mu k^2 / \mu_t \tag{5}$$

In this formula, the density is found from a perfect gas (dry air) equation of state, k is from the Mellor-Yamada-Janjic model, and μ_t is the momentum diffusion coefficient.

Imposition of WRF Pressure Gradient

We impose the WRF pressure gradient onto the CFD model by finding the difference in the imposed WRF pressure from the local pressure that would be present in an ideal atmosphere for the WRF ground base state, and supply this pressure difference on the boundaries of the CFD model. Furthermore, we operate the CFD model in an isothermal, constant density mode, where we have not imposed gravitational body force terms in the vertical momentum equation. For this study,

this approach is found to be preferable to running the CFD solver in a compressible mode including the gravitational body force, since it was found that directly coupling it to the thermodynamic field from the mesoscale model has a number of disadvantages. If a direct coupling is made, both models must have consistent thermodynamic models (including humidity transport and equations of state), as well as having similar air to ground heat transfer models. Small differences in these thermodynamic quantities can produce spurious flow behavior in the CFD model. After a series of computations, we determined that a pragmatic approach that was taken for this study is to apply the difference of the local WRF pressure to that of an ideal atmosphere, which the CFD model uses as the pressure difference from the (constant) CFD reference pressure. That is, impose on the face-centers of the CFD mesh:

$$\Delta P = P_{WRF.G} - P_b \left[1 - \frac{1}{\kappa} \frac{g}{RT_b} (z - z_b) \right]^\kappa \quad (6)$$

The base state variables (P_b, T_b) and base height (z_b) are found via interpolation of the WRF data on the ground surface given the (x,y) coordinate of the CFD mesh boundary face above it, while $P_{WRF.G}$ is the pressure from the WRF data interpolated to the CFD boundary face.

Unsteady Coupling
The unsteady coupling mode operates the CFD solver in an unsteady fashion, and linearly interpolates the WRF data in time from 15 minute storage intervals. This approach is quite costly, as the CFL restrictions limit the allowable time step to be much lower than the mesoscale model time step, and the CFD solver must solve the mass constraint, momentum conservation and turbulence model equations at each time step. The contaminant transport equation is solved in an unsteady mode, along with the other model equations.

"Quasi-Steady" Coupling
The quasi-steady mode first computes the steady state, equilibrium, flow fields at 15 minute intervals, using the WRF data as boundary conditions. The unsteady, contaminant transport evolution equation is then solved using the quasi-steady velocity and turbulence field that is found by linearly interpolating the appropriate steady state fields in time. We call this collection of steady-state wind fields a "wind field library", and the blending of these wind fields in time to solve

the contaminant transport equation, the "unified frozen hydrodynamic solver".

5. MODEL ASSESSMENT STUDY

To assess the model accuracy, we have first performed baseline calculations using sounding data taken during the field test, as this mode of operation is commonly used when performing CFD calculations in the absence of mesoscale model data. Next, we assess the unsteady and quasi-steady coupling strategies.

a. CFD Model Mesh and Configurations
The CFD model mesh is constructed using a quadtree-prismatic/octree, Cartesian mesh generator that is embedded in a solution adaptive flow solver [Coirier et al., 2002, 2006.a]. Two different meshes are used in the study: a coarse and a fine mesh. Both meshes cover a domain of 8.4 by 7.4 by 1 kilometers. The coarse mesh has approximately 325,000 cells with a lateral resolution of approximately 20 meters in the CBD growing to approximately 200 meters near the domain boundaries. The fine mesh has approximately 1,300,000 cells, where the resolution is approximately 10 meters in the CBD and grows to 100 meters near the domain boundaries. Both meshes have the same clustering normal to the ground plane, which has a resolution of 1 meter near the ground, and grows smoothly to approximately 40 meters near the upper boundary. Computational cells that lie completely within buildings are removed, while buildings that occupy partial cells are modeled using the drag model. Digital elevation data is used to map the constant height ground plane mesh to be conformal to the terrain using a displacement model. Figure 2 shows an overview of the ground surface of the coarse mesh.
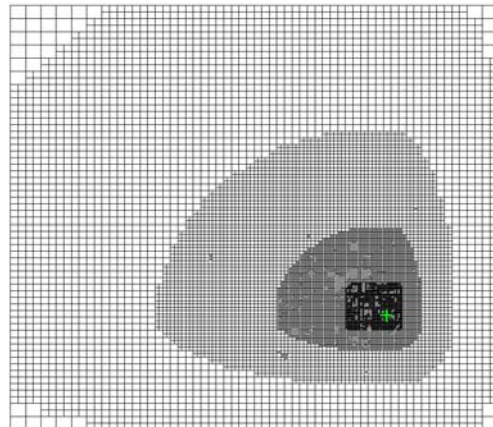
Figure 2: Surface mesh of coarse grid model.

b. Isolated Mode: Raging Waters Input

The Raging Waters meteorological data site was used to supply boundary conditions of velocity and turbulence for CFD-Urban. There are significant deficiencies when using this sounding data: There is only one measurement location, which is inadequate for the domain size considered here. There is no pressure data to apply at the boundaries. (We note the importance of this externally supplied pressure gradient in the coupled calculations in subsequent sections.) The turbulence data is inconsistent in that it is either missing or is far from being in equilibrium with the inconsistent wind speed profiles, which are themselves non-smooth when composited together into a single profile. Furthermore, when applying turbulence equilibrium theory to supply turbulence quantities using the velocity gradient data, the non-smooth velocity profiles produce unrealistic turbulence quantities. To overcome the lack of consistent turbulence model data we use a Monin-Obukhov Similarity (MOS) [Obukhov, 1971] profile with: $u_* = 0.35$ m/s, $z_o = 0.55$ m, and a similarity length scale of 80m. This is found by a best visual fit of the MOS profile with the (composited) supplied wind profile data. For the wind direction, we directly use the measured data either at the different time intervals or as an average.

Unsteady and quasi-steady calculations were made using the Raging Waters Site input data, as described above, and the statistics shown in equations 1 to 4 are used to quantify the model accuracy. Plots of predicted versus measured concentrations are made, where the lines indicating the factor of two bounds are drawn.

5.1 Raging Waters, Unsteady Mode Results

Calculations using the unsteady mode were made, and after postprocessing, yielded the results shown in Figure 3 and Table 1.

5.2 Raging Waters, Steady Mode Results

Calculations using the quasi-steady mode were made, and after postprocessing, yielded the results shown in Figure 4 and Table 2. Since there is only a single unsteady boundary condition set of data, these mode of calculation is more appropriately termed as a steady mode.

a. Downscale WRF Data: Unsteady Mode

The dispersion modeling accuracy statistics and scatter plots are shown in Figure 5 and Table 3 below for the unsteady mode of operation using the WRF downscale transferred data at 15 minute intervals.

b. Downscale WRF Data: Quasi-Steady Mode

The statistical results and scatter plots for the quasi-steady mode of operation are shown here in Figures 6, 7 and 8 and Tables 4, 5 and 6, for the WRF/Noah model using the coarse and fine grids, as well as results for the WRF/Noah-UCM model on the coarse grids.

c. Downscale WRF/Noah Quasi Steady, Coarse Grid

The results using the quasi-steady mode of operation, applying the downscale data from the WRF/Noah model on the coarse CFD grid are shown in Figure 6 and Table 4.

5.3 Downscale Wrf/Noah, Quasi-Steady, Fine Grid

The results using the quasi-steady mode of operation, applying the downscale data from the WRF/Noah model on the fine CFD grid are shown in Figure 7 and Table 5.

5.4 WRF/Noah-UCM, Quasi-Steady, Coarse Grid

Finally, the results using the quasi-steady mode of operation, applying the downscale data from the WRF/Noah-UCM model on the coarse CFD grid are shown in Figure 8 and Table 6.

6. CONCLUSIONS

Based upon this study we make the following conclusions:

The unsteady mode of operation is not recommended as an operational mode of coupling NWP and CFD models. Although it is feasible that with enough computational resources the two might be coupled so that they operate in a temporally synchronized manner, the time step restrictions (based upon the CFL condition in the CFD component) will result in a large computational overhead that is difficult to overcome. This could be alleviated somewhat by using larger cells (ie.: less resolution) in the CFD mesh, but this would defeat one of the purposes of performing the CFD calculations.

On the other hand, we strongly recommend using the quasi-steady mode of operation. The statistical measures of the transport and dispersion modeling accuracy have shown that this mode can produce quantifiably improved results over the isolated sounding data (Raging

Waters) mode and the unsteady mode. From a computational coupling aspect, this mode is also preferred for the following reasons.

Operational Wind Field Library Generation: The steady state (equilibrium) urban wind fields can be computed relatively quickly, and stored for subsequent re-use in wind field libraries. When used operationally (as shown in Section 7), the production of these wind fields using the latest NWP or assimilated data as boundary conditions can be interleaved with the NWP model computations and/or data assimilation models themselves.

Fast Contaminant Transport Calculations: Using the Unified Frozen Hydrodynamics Solver approach coupled with the wind libraries generated by using the latest data from from the NWP models, fast contaminant transport calculations can be made.

The potential benefits of up-scale data transfer needs to be assessed, as well as precisely what data to transfer, when to transfer it and how to transfer it. Before this can be accomplished, a computational framework is needed to embed both the CFD and NWP models, allowing a more practical means to investigate the different types of data and transfer modes. One potential framework to perform this coupling is the Earth System Modeling Framework [Hill, et al., 2004].

In addition, we conclude that to couple the CFD model with the NWP model, it is best to formulate the equations that the CFD component solves to be more consistent with the physics used in the NWP solver. This should include, and not necessarily be limited to, accounting for a non-dry air equation of state, solving for an energy equation (formulated using the potential temperature), as well as formulating the mass conservation via the pressure correction approach to use the deviation of pressure from the ideal hydrostatic pressure variation. Additional turbulence closures need to be addressed, using formulations based on PBL models, such as the Mellor-Yamada-Janjic model.

7. QUASI-STEADY, OPERATIONAL COUPLING

Based upon our study, we find that the mode of operation we consider most promising is to operate both the CFD and NWP models in a "hot" (concurrently running) mode, where for a given simulation time period (say, 15 minutes simulated time), the following sequences of operations occur in a repeated, synchronized manner:

Downscale Data Transfer: The latest results from the NWP model, such as WRF, are processed, and used to supply the latest boundary condition data to the CFD model. This data may be generated in either a time-accurate or lagged fashion.

CFD Convergence: Given the downscale data, the CFD model is hot restarted, from the previously converged solution, and converges to the solution corresponding to the latest downscale data.

Upscale Data Transfer: The CFD results are processed, and provide the upscale data needed in the NWP model, which is transferred to the NWP model.

NWP Time Advance: The NWP model advances through time using the latest data in either a lagged or predictor manner.

This mode of operation is similar to the operational model for the Pentagon Shield system [Warner, 2006], where CFD-Urban is cycled at appopriate time intervals, receiving new boundary condition data from the data assimilation systems, and updating building surface pressure and gridded velocity and turbulence field data.

8. RECOMMENDATIONS

This study illustrates the potential benefit of employing a mesoscale Numerical Weather Prediction forecast to drive microscale CFD-urban models. Based upon our study, we recommend using a quasi-steady means to couple Numerical Weather Prediction models such as WRF to Computational Fluid Dynamic models for urban areas. Furthermore, we recommend embedding both the CFD and NWP model within a software architecture, such as the Earth System Modeling Framework, to sychronize the models, and to provide a data exchange protocol to transfer and manipulate the data between them. In addition, we recommend formulating the CFD model governing equations to use physics more consistent with the NWP models physics. This will lay the framework from which the upscale data transfer can be formulated and assessed, in order to improve the modeling accuracy of the NWP models. By performing this integration within the ESMF, other ESMF compatible NWP models may directly benefit from this work.

9. ACKNOWLEDGEMENTS

10. REFERENCES

ACE+, V2003 Users Manual, Volumes 1 and 2.

Allwine, K.J., J.H.Shinn, G.E. Streit, K.L. Clawson, M.Brown, 2002, Overview of Urban 2000. *Bull. Am. Meteorol. Soc.*, **83** (4), 521-536.

Chen, F., and J. Dudhia, 2000: Coupling an advanced land-surface/hydrology model with the Penn State/NCAR MM5 modeling system. Part I: Model implementation and sensitivity. *Mon. Wea. Rev.*, **129**, 569-585.

Coirier, W.J., et al., 1998: CFD-DTF: A data transfer facility for CFD and multidisciplinary analysis, AIAA-98-0125.

Coirier, W.J., Furmancyzk, M., Przekwas, A.J.,2002 Development of an Image- and CFD-Based Urban Scale Wind Field and Dispersion Simulator, American Meteorological Society, 4th Symposium on the Urban Environment, p. J17, J1.11.

Coirier, W., Reich, A., Fricker, D., Furmanczyk, M., Przekwas, A., 2003.a: *Application of CFD-Urban For Support of the Joint URBAN 2003 Field Test*, 7th Annual George Mason University Conference on Transport and Dispersion, Fairfax, Virginia.

Coirier, W.J., Fricker, D.M., and Furmanczyk, M.: 2003.b, Development of a high fidelity PC based simulator for modeling the atmospheric transport and dispersion of nuclear, chemical, biological and radiological substances in urban areas, DTRA SBIR Phase II Final Report: Contract: DTRAA01-01-0079.

Coirier, W., Kim, S., 2004: *Validation of CFD-Urban using Accepted Open Field and Urban Area Transport and Dispersion Test Data*. 8th Annual George Mason University Conference on Transport and Dispersion Modeling, July 13-15, Fairfax, Virginia.

Coirier, W.J., Fricker, D.M., Furmanczyk, M., and Kim, S., 2005.a,"A Computational Fluid Dynamics Approach for Urban Area Transport and Dispersion Modeling", in print, Environmental Fluid Mechanics, Vol. 15(5).

Coirier, W.J., Kim, S., 2005.b: Detailed transport and dispersion calculations in support of the MSG05 field test, 9th Annual George Mason University Conference on Transport and Dispersion Modeling, July 18-20, Fairfax, Virginia.

Coirier, W.J., Kim, S.K, 2006.a, CFD Modeling for Urban Area Contaminant Transport and Dispersion: Model Description and Data Requirements, American Meteorological Society, 6th Symposium on the Urban Environment, 2006.

Coirier, W.J., Kim, S.K, 2006.b, Summary of CFD-Urban Results in Support of the Madison Square Garden and Urban Dispersion Program Field Tests, American Meteorological Society, 6th Symposium on the Urban Environment, 2006.

Dudhia, J., 1989: Numerical study of convection observed during the winter monsoon experiment using a mesoscale two-dimensional model. *J. Atmos. Sci.,* 46, 3077-3107.

Hill, C., et al. 2004: The architecture of the earth system modeling framework. *Computing in Sciency and Eng,* **6**:1.

Janjic, Z. I., 2002: Nonsingular Implementation of the Mellor-Yamada Level 2.5 Scheme in the NCEP Meso model. NCEP Office Note No. 437, 61.

Jiang, Y., Przekwas, A.J.: 1994. Implicit, pressure-based incompressible Navier-Stokes solver for unstructured meshes, AIAA-94-0303.

Jiang, Y., Fricker, D.M., Coirier, W.J., 1999: Parallelization of a fully implicit unstructured pressure-based flow solver using MPI, AIAA-99-3274.

Kain, J. S., and J. M. Fritsch, 1993: Convective parameterization for mesoscale models: The Kain-Fritcsh scheme. The representation of cumulus convection in numerical models, K. A. Emanuel and D.J. Raymond, Eds., Amer. Meteor. Soc., **246**.

Kusaka, H., H. Kondo, Y. Kikegawa, and F. Kimura, 2001: A simple single-layer urban canopy model for atmospheric models: Comparison with multi-layer and slab models. *Bound.-Layer Meteorol.*, 101, 329-358

Launder, B.E. and Spalding, D.B., 1974: The numerical computation Of turbulent flows, *Computer Methods In Applied Mechanics And Engineering.* **3**, 269-289.

Liu, J., Chen, J.M., Black, T.A., Novak, M.D., 1996: "*E-Epsilon Modeling of Turbulent Air Flow Downwind of a Model Forest Edge*", Boundary-Layer Meteorology, V 77, pp 21-44.

Liu et al. (2005): Verification of a mesoscale data assimilation and forecasting system for the Oklahoma City area during the joint urban

2003 field project. Submitted to *J. Appl. Meteor*.

Marshall, R.E., Meris, R.G. and Hannan, J.R., 2004: Uncertainty in the prediction of atmospheric transport of chemical, biological, radiological, and nuclear (CBRN) hazards, Summary Rpt.

Mellor, G. L., & T. Yamada, 1974: A hierarchy of turbulence closure models for planetary boundary layers. *J. Atmos. Sci.*, **31**, 1791-1806.

Mlawer, E. J., S. J. Taubman, P. D. Brown, M. J. Iacono, and S. A. Clough, 1997: Radiative trans-fer for inhomogeneous atmosphere: RRTM, a validated correlated-k model for the long-wave. *J. Geophys. Res.,* **102**(D14), 16663-16682.

NetCDF: NetCDF Users' Guide. Version 3.6.1.

Obukhov, A.M, 1971: Turbulence in an atomspher with non-uniform temperature. Boundary-Layer Meteorolgy., **2**, 7-29.

OFCM, 2004: Federal research and development needs and priorities for atmospheric transport and diffusion modeling.

urban.llnl.gov: Urban 2000 Web Site, Data Link, http://urban.llnl.gov .

Warner, T.T, 2006: An operational building-scale urban forecasting system: Pentagon Shield", 6th Symposium on the Urban Environment, J4.2.

Weil, J.C., Sykes, R.I., and Venkatram, A.: 1992, Evaluating air-quality models: review and outlook, *Journal of Applied Meteorology*, 31, 1121-1145.
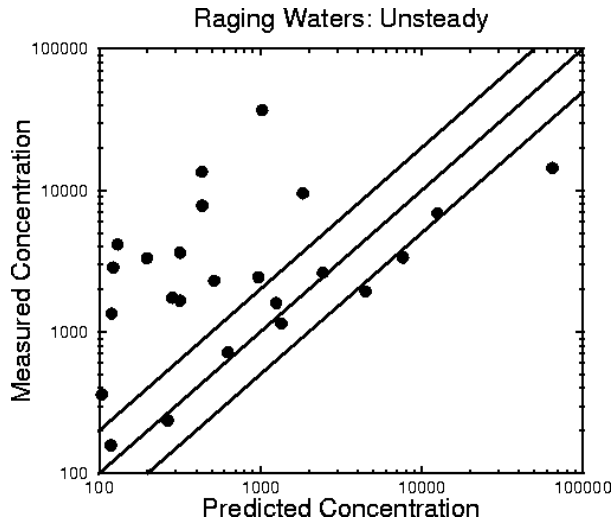
Figure 3: Raging Waters, unsteady mode measured versus predicted concentrations.

	Near Source	R2	R3	R4	All
FB	0.85	1.59	1.44	1.7	0.87
NMSE	14.03	15.8	14.4	26.1	21.9
MG	25.42	14.1	4.58	5.06	15.8
FAC2	0.12	0.17	0.36	0.38	0.18

Table 1: Raging Waters, unsteady mode statistical measures of transport and dispersion modeling accuracy.
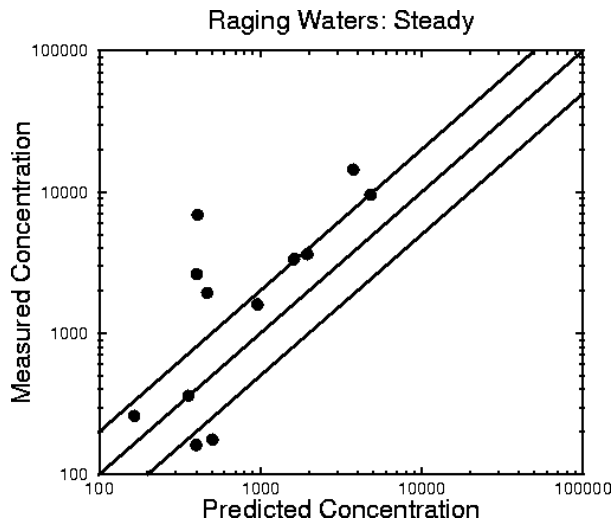
Figure 4: Raging Waters, steady mode measured versus predicted concentrations.

	Near Source	R2	R3	R4	All
FB	1.77	1.49	1.5	1.74	1.76
NMSE	61.41	12	17.5	31.7	92
MG	78.84	15.4	5.12	5.67	33.3
FAC2	0.08	0.25	0.45	0.38	0.18

Table 2: Raging Waters, steady mode statistical measures of transport and dispersion modeling accuracy.

WRF/Noah: Unsteady
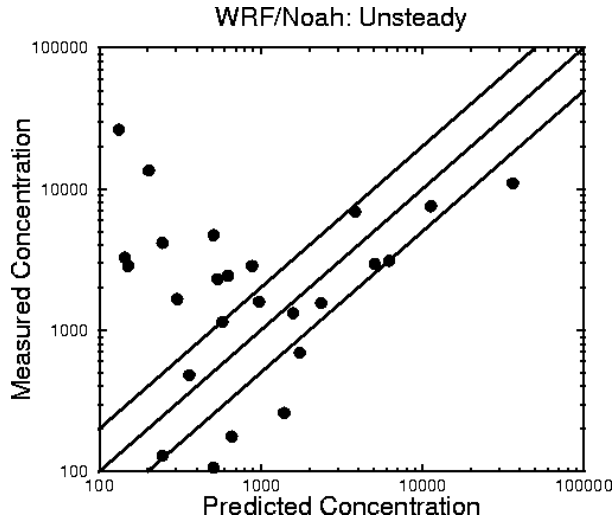
Figure 5: Downscale WRF Data Transfer, unsteady mode measured versus predicted concentrations.

Table 3: Downscale WRF Data Transfer, unsteady mode statistical measures of transport and dispersion modeling accuracy.
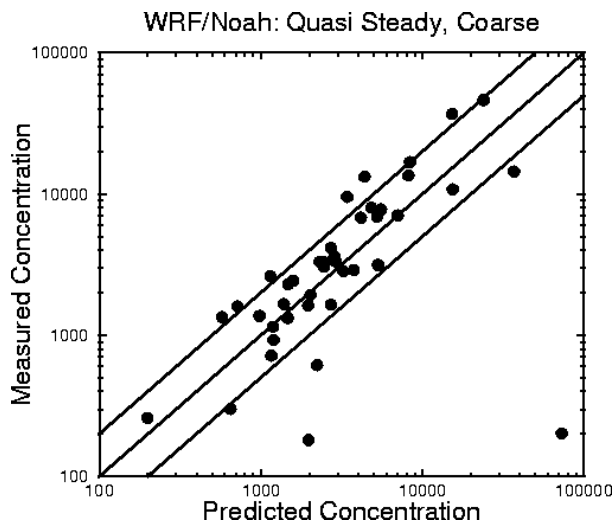
	Near Source	R2	R3	R4	All
FB	1.56	1.66	1.59	1.74	1.57
NMSE	30.56	19.8	22.2	31.7	47.3
MG	15.89	11.6	4.77	5.68	11.7
FAC2	0.08	0.17	0.36	0.38	0.16

WRF/Noah: Quasi Steady, Coarse

Figure 6: Downscale WRF/Noah, quasi-steady mode, coarse CFD grid, measured versus predicted concentrations.

Table 4: Downscale WRF/Noah, quasi-steady mode, coarse CFD grid, statistical measures of transport and dispersion modeling accuracy.

	Near Source	R2	R3	R4	All
FB	-0.77	0.4	0.8	0.8	-0.76
NMSE	34.36	1	2.3	1.8	53.7
MG	0.74	1.6	2	2.1	1.04
FAC2	0.57	0.4	0.4	0.5	0.51

WRF/Noah: Quasi–Steady, Fine
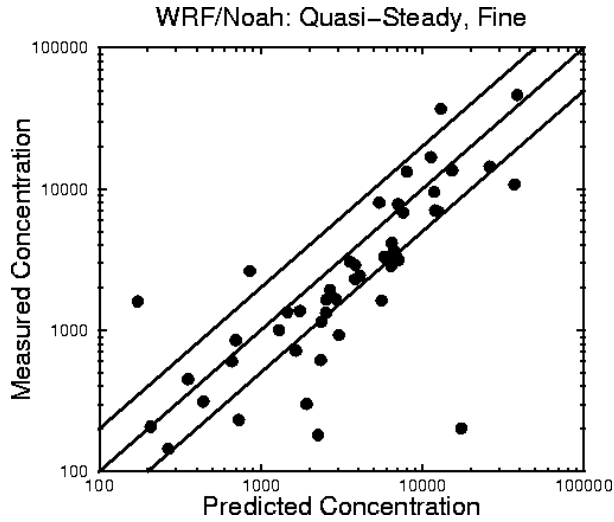
Figure 7: Downscale WRF/Noah, quasi-steady mode, fine CFD grid, measured versus predicted concentrations.

Table 5: Downscale WRF/Noah, quasi-steady mode, fine CFD grid, statistical measures of transport and dispersion modeling accuracy.

	Near Source	*R2*	*R3*	*R4*	*All*
FB	-1.35	-0.2	0.1	0.9	-1.34
NMSE	147.98	0.65	0.6	2.6	232
MG	0.53	1.6	1.9	2.4	0.8
FAC2	0.51	0.42	0.6	0.4	0.5

WRF/Noah–UCM: Quasi–Steady
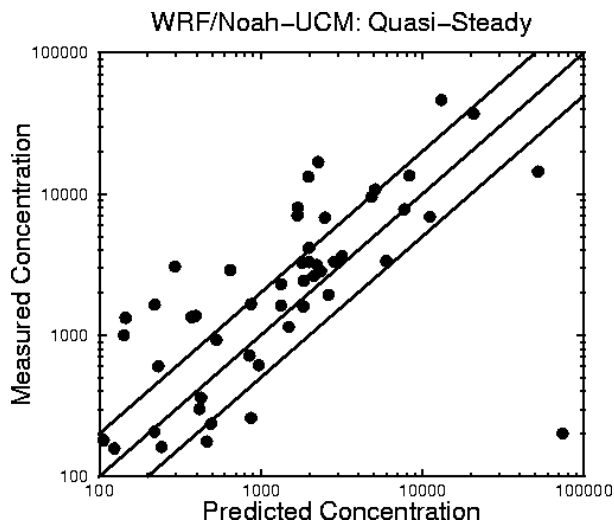
Figure 8: Downscale WRF/Noah-UCM, quasi-steady mode, coarse CFD grid, measured versus predicted concentrations.

Table 6: Downscale WRF/Noah-UCM, quasi-steady mode, coarse CFD grid, statistical measures of transport and dispersion modeling accuracy.

	Near Source	*R2*	*R3*	*R4*	*All*
FB	-0.79	0.8	1.1	1.3	-0.78
NMSE	41.7	3.2	6.6	7.2	65.3
MG	1.06	3.6	2.7	3.3	1.51
FAC2	0.51	0.3	0.5	0.4	0.45